

Diffusion Mechanism of Exciplexes in Organic Optoelectronics

Hwang-Beom Kim¹ and Jang-Joo Kim^{1,2,*}

¹*Department of Materials Science and Engineering, Seoul National University, Seoul 151-742, South Korea*

²*Research Institute of Advanced Materials (RIAM), Seoul National University, Seoul 151-744, South Korea*

 (Received 23 June 2019; revised manuscript received 30 October 2019; accepted 7 January 2020; published 5 February 2020)

Excited-state charge-transfer complexes (exciplexes) are actively exploited in organic optoelectronics to understand their nature in the solid state and improve device performance. However, the diffusion of exciplexes is not actively studied, despite its ever-growing importance in such devices due to the lack of apparent charge-transfer (CT) absorption. Here, we report, based on time-resolved photoluminescence spectroscopy, that energy transfer (ET) takes place directly from exciplexes to exciplexes; this is called exciplex-exciplex ET. Recent reports and our own observation of the subband-gap CT absorption in exciplex-forming systems support the direct exciplex-exciplex ET. The ET takes place dominantly via the Dexter-type exchange mechanism, as revealed by the exponential decrease of the ET rate constant with separation between the energy-donating exciplex and the energy-accepting exciplex.

DOI: [10.1103/PhysRevApplied.13.024006](https://doi.org/10.1103/PhysRevApplied.13.024006)

I. INTRODUCTION

Excited-state charge-transfer complexes (exciplexes) are formed by partial charge transfer in the excited state between electron-donor molecules and nearby electron-acceptor molecules after photoexcitation of the molecules [1,2]. Exciplexes are widely observed in nature, such as photosynthetic systems, and organic optoelectronic devices, such as organic photovoltaics (OPVs) or organic light-emitting diodes (OLEDs), where heterojunctions between electron-donor and -acceptor molecules are employed. Exciplexes have long been considered as an obstacle because they have low emission efficiency in OLEDs and reduce the dissociation probability of charge-transfer (CT) states in OPVs. Recently, however, exciplexes have been actively used as thermally assisted delayed fluorescence (TADF) emitters in OLEDs to take advantage of their higher luminescent exciton ratio, due to their small energy difference between the singlet and triplet excited states [3–6]. Exciplexes are also used as host materials in highly efficient OLEDs, exploiting low driving voltage, good charge balance, and low-efficiency roll-off [7–9].

Exciplexes are known for a new emission band that is redshifted from molecular emission bands, but the absence of the absorption band for the exciplex state when electron donors and acceptors are close together [1,2]. The formation, electronic structure, and excited-state dynamics of exciplexes in films have been actively researched in recent years [1,4,5,10–17]; however, the diffusion of exciplexes

has not been studied until very recently, primarily because of the lack of apparent CT absorption in exciplex-forming systems measured by standard steady-state absorption experiments, which is a necessary condition for diffusion to take place via energy-transfer (ET) mechanisms. The lack of apparent CT absorption in standard steady-state absorption experiments in exciplex-forming systems is the reason for the term “exciplex” [2].

There are papers describing the diffusion of exciplex or polaron pairs. Deibel and co-workers suggest that the diffusion of polaron pairs might account for efficiency loss in OPVs by applying Monte Carlo simulations [18]. Baldo *et al.* report that CT exciplex states can be transported via an “inchworm” mechanism [19]. The spatial distribution of the photoluminescence (PL) intensity of exciplexes over the decay time of CT exciplex states is measured and the diffusion of exciplexes is confirmed. This phenomenon is explained through geminated charge recombination at different sites, from which CT exciplex states are initially formed. The movement distance of CT exciplex states is in the range 5–10 nm for about 20 μ s. It is discussed that Förster-type resonance energy transfer (FRET) for the diffusion of CT exciplex states will not be effective because of the negligibly low optical absorption of CT exciplex states and that Dexter-type exchange energy transfer (DET) will also not be effective because CT exciplex states are weakly bound.

Here, we report that there is not one single mechanism for exciplex diffusion and that DET is the dominant mechanism based on the analysis of time-resolved PL measurements of high-energy exciplexes and low-energy exciplexes. Even though the CT absorption is orders of

*jjkim@snu.ac.kr

magnitude weaker than that of the normal resonance absorption [20–25], recent reports and our own observation for the subband-gap CT absorption in organic electron donor-acceptor systems support that exciplex-exciplex ET takes place. The exciplex-exciplex ET means that ET from exciplex 1 to exciplex 2. In that case, exciplex 1 loses its excitation energy and exciplex 2 is generated from the ground state near exciplex 1. When D and A represent the electron-donor and -acceptor molecules, respectively, and δ is the degree of CT in the exciplex state, the exciplex-exciplex ET could be described by $[(D_1^{\delta_1+} A_1^{\delta_1-})^* + (D_2 A_2) \rightarrow (D_1 A_1) + (D_2^{\delta_2+} A_2^{\delta_2-})^*]$, where $(D_1^{\delta_1+} A_1^{\delta_1-})^*$ and $(D_2^{\delta_2+} A_2^{\delta_2-})^*$ represent exciplex 1 losing its excitation energy and exciplex 2 gaining its excitation energy, respectively.

II. EXPERIMENTS

Four donor molecules of 4,4'-bis(3-methylcarbazol-9-yl)-2,2'-biphenyl (mCBP), di-[4-(*N,N*-ditolylamino)phenyl]cyclohexane (TAPC), tris(4-carbazoyl-9-ylphenyl)amine (TCTA), and 4,4',4''-tris(3-methylphenylphenylamino)triphenylamine (m-MTDATA) and one acceptor molecule of (1,3,5-triazine-2,4,6-triyl)tris(benzene-3,1-diyl)tris(diphenylphosphine oxide) (PO-T2T) are used as the exciplex-forming materials. They are purchased from Nichem Fine Technology and used as received without further purification. All organic films are deposited by thermal evaporation at a rate of 1 \AA s^{-1} on precleaned quartz substrates under vacuum at a base pressure of $< 5 \times 10^{-7}$ Torr. Extinction coefficients are measured using variable-angle spectroscopic ellipsometry (VASE, J. A. Woolam M-2000 spectroscopic ellipsometer). A spectrofluorometer (Photon Technology International, Inc.) with an incorporated monochromator (Acton Research Co.) is used for steady-state PL spectra measurements. A nitrogen gas laser with an excitation wavelength of 337 nm (3.68 eV) and a pulse width of 800 ps (KEN-2X, Usho), combined with a streak camera (C10627, Hamamatsu Photonics), is used for time-resolved PL experiments.

III. RESULTS

A. ET from high-energy exciplexes to low-energy exciplexes

We conduct two different experiments to investigate ET from exciplexes to other kinds of exciplexes. The first experiment exploits a bilayer system with two different kinds of exciplexes. The second one is carried out for a codoped system with two different kinds of exciplexes, where two different kinds of electron-donor molecules are codoped (5 mol % each) into an electron-acceptor host.

First, an exciplex-forming TAPC/PO-T2T mixed film (1:1 molar ratio, 2 nm thick) is stacked on another exciplex-forming mCBP/PO-T2T mixed film [1:1 molar

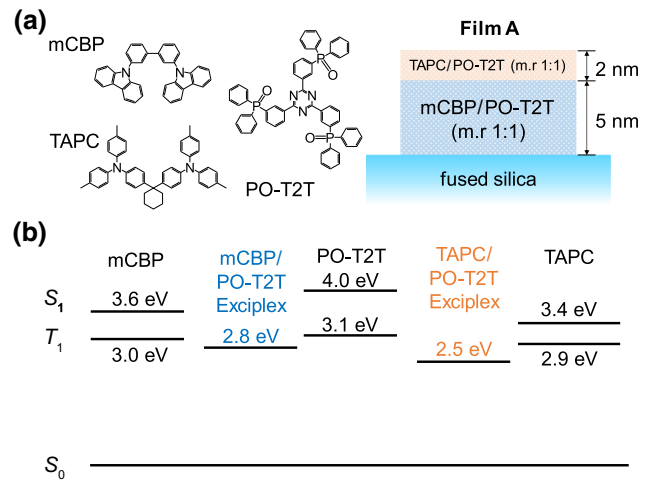


FIG. 1. (a) Molecular structures of mCBP, TAPC, and PO-T2T and bilayer structure of film A. (b) Energy levels of mCBP, TAPC, and PO-T2T excitons and mCBP/PO-T2T and TAPC/PO-T2T exciplexes in the films, where S_1 and T_1 represent the lowest excited singlet and triplet excited states, respectively.

ratio, 5 nm thick; film A in Fig. 1(a)], and the emission characteristics of the bilayer film are compared with those of the nonstacked single-layer films. The structures for molecules in the films are shown in Fig. 1(a). The energy levels of the mCBP, TAPC, and PO-T2T excitons, and the mCBP/PO-T2T and TAPC/PO-T2T exciplexes, are shown in Fig. 1(b). Formation of exciplexes in the mCBP/PO-T2T and TAPC/PO-T2T films is confirmed by the featureless redshifted emission from the constituent materials, as shown in Fig. 2 [26,27]. mCBP and TAPC are used as electron donors and PO-T2T is used as an electron acceptor for the exciplexes. The thickness of the films is

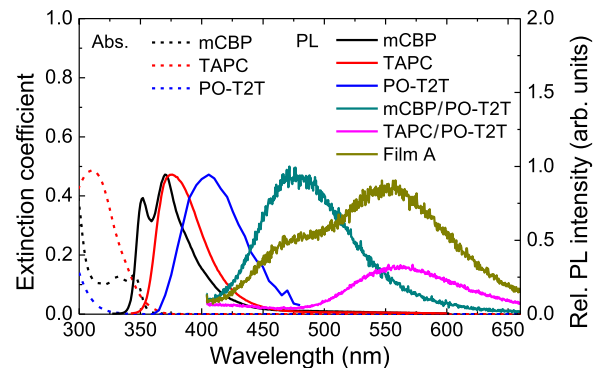


FIG. 2. Extinction coefficients of mCBP, TAPC, and PO-T2T films; steady-state PL spectra of mCBP film, TAPC solution in dichloromethane at 10^{-4} M, and PO-T2T solution [27]; and time-resolved PL spectra of mCBP/PO-T2T film (5 nm thick), TAPC/PO-T2T film (2 nm thick), and film A integrated for 9 μ s after excitation at 337 nm.

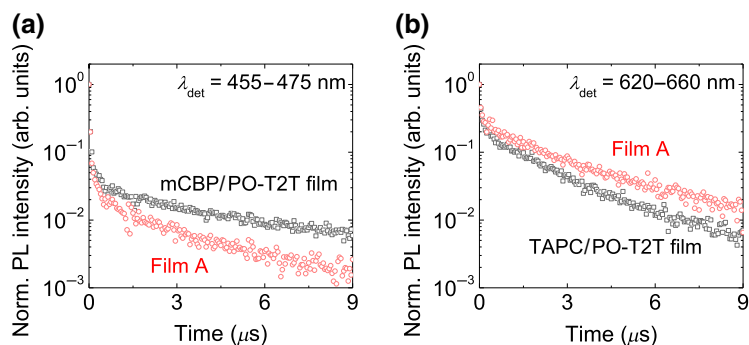


FIG. 3. (a) Normalized transient PL intensities for mCBP/PO-T2T film [molar ratio (m.r.) 1:1] and film A in the wavelength range of 455 to 475 nm (semilogarithmic plot). (b) Those for TAPC/PO-T2T (m.r. 1:1) film and film A in the wavelength range of 620 to 660 nm (semilogarithmic plot).

adjusted for clear observation of the interface quenching effect (or ET) in the transient PL experiments. If the films are too thick, the interface quenching effect will be buried by a strong bulk effect because the interface effect is limited at the interface no matter how thick the films are. If they are too thin, the signal must be too small to clearly detect. Figure 2 also compares the time-resolved emission spectra integrated for 9 μs after excitation when the films are excited with a N_2 pulsed laser (337 nm wavelength with a pulse width of 0.8 ns). The emission from the bilayer film is composed of the exciplex emissions from the constituent layers. The longer wavelength emission from the TAPC/PO-T2T layer, with a peak wavelength of 560 nm, is significantly increased and the exciplex emission from the mCBP/PO-T2T layer, with a peak wavelength of 475 nm, is reduced significantly in film A compared with that of the single-layer emissions. The energy levels of the mCBP, TAPC, and PO-T2T singlet excitons are estimated from the onset of their absorption spectra. The energy levels of the mCBP, TAPC, and PO-T2T triplet excitons and mCBP/PO-T2T and TAPC/PO-T2T singlet exciplexes are estimated from the onset of their integrated emission spectra. The triplet energy levels of exciplexes are similar to the singlet levels due to small overlap between the highest occupied molecular orbital (HOMO) and the lowest unoccupied molecular orbital (LUMO) because they are mainly located in different materials, i.e., the HOMO in the donor molecule and the LUMO in the acceptor molecule, respectively [4,28–30]. The normalized transient PL intensities from the single layers are compared with those of the bilayer for the mCBP/PO-T2T exciplex emission (detection wavelength 455–475 nm) and the TAPC/PO-T2T exciplex emission (detection wavelength 620–660 nm) in Figs. 3(a) and 3(b), respectively, which are semilogarithmic plots. The results show that the lifetime of the delayed emission of the mCBP/PO-T2T exciplex in the stacked layer is significantly reduced relative to that of the single layer. In contrast, the lifetime of delayed emission from the TAPC/PO-T2T exciplex in the stacked layer is significantly increased compared with that of the single layer. The transient results show that ET takes place from the mCBP/PO-T2T exciplex to the TAPC/PO-T2T exciplex.

Similar behavior is observed in a different exciplex-forming system, where two electron-donor molecules (TCTA and m-MTDATA) are codoped in an electron-acceptor host (PO-T2T) at 5 mol% each [film B in Fig. 4(a)]. The molecular structures of TCTA and m-MTDATA are shown in Fig. 4(a). The energy levels of the system are shown in Fig. 4(b) and are estimated using the same methods as those in Fig. 1(b). The featureless redshifted emission spectra of the mixed films of TCTA/PO-T2T and m-MTDATA/PO-T2T in Fig. 5 confirm the formation of exciplexes between TCTA or m-MTDATA and PO-T2T. The extinction coefficients of TCTA, m-MTDATA, and PO-T2T neat films and m-MTDATA/PO-T2T (m.r. 1:1) mixed film [31] are shown in Fig. 5, along with the time-resolved emission spectra of a TCTA/PO-T2T (m.r. 5:95) doped film, an m-MTDATA/PO-T2T (m.r. 5:95) doped film, and film B integrated for 500 ns after excitation, when the electron donors in the films are selectively excited by a N_2 pulsed laser at the wavelength of 337 nm. Again the emission from film B

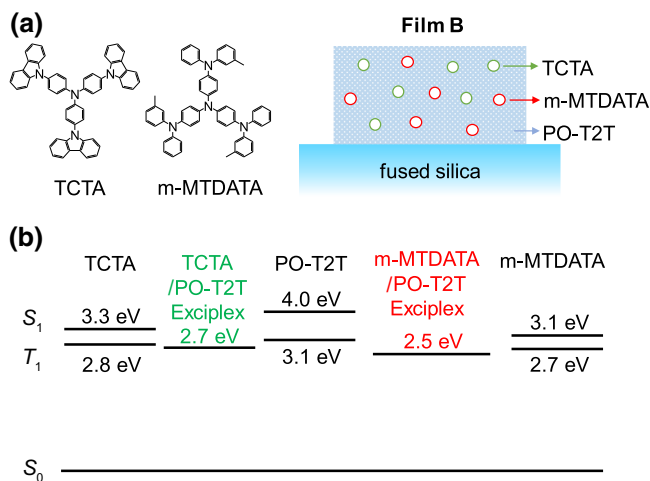


FIG. 4. (a) Molecular structures of TCTA, m-MTDATA, and PO-T2T film codoped with TCTA and m-MTDATA (film B). (b) Energy levels of S_1 and T_1 of TCTA, m-MTDATA, and PO-T2T excitons and TCTA/PO-T2T and m-MTDATA/PO-T2T exciplexes in the films.

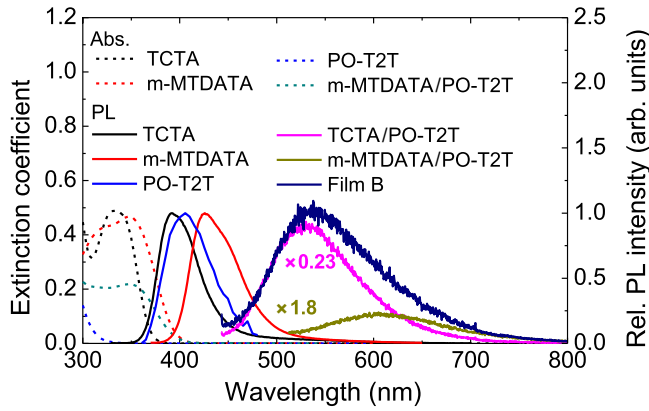


FIG. 5. Extinction coefficients of TCTA, m-MTDATA, PO-T2T, and m-MTDATA/PO-T2T (m.r. 1:1) films; steady-state PL spectra of a TCTA film, m-MTDATA film, and PO-T2T solution [27]; and time-resolved PL spectra integrated for 500 ns after excitation of TCTA/PO-T2T (m.r. 5:95) film ($\times 0.23$), m-MTDATA/PO-T2T (m.r. 5:95) film ($\times 1.8$), and film B.

is composed of the emissions from the TCTA/PO-T2T exciplexes and m-MTDATA/PO-T2T exciplexes, which are the high-energy exciplexes and low-energy exciplexes, respectively. The intensity of the TCTA/PO-T2T exciplex in film B is significantly reduced to 23% compared with the singly doped TCTA/PO-T2T (m.r. 5:95) film and the m-MTDATA/PO-T2T exciplex emission increases to 1.8 times that of the singly doped film. These results indicate that the energy is transferred from the excited states involving TCTA molecules to those involving m-MTDATA molecules, considering the energy levels of the singlet excitons of TCTA and m-MTDATA and the singlet exciplexes of TCTA/PO-T2T and m-MTDATA/PO-T2T. Figure 6(a) compares the transient PL profiles on a semilogarithmic scale of the TCTA/PO-T2T exciplex emission from film B to that from the singly doped TCTA/PO-T2T film measured in the wavelength range 510 to 530 nm, where the TCTA/PO-T2T exciplex emission is dominant. The decay rate constant for the emission of the TCTA/PO-T2T exciplexes in film B is faster than that in the singly doped TCTA/PO-T2T film. On the other hand,

the decay rate constant of the m-MTDATA/PO-T2T exciplexes in film B is slower than that in the singly doped m-MTDATA/PO-T2T film in the detection-wavelength range of 700 to 800 nm, where the m-MTDATA/PO-T2T exciplex emission is dominant, as shown in Fig. 6(b) as semilogarithmic plots.

The reduction of the lifetime and intensity of the high-energy exciplex PL and the increase of the low-energy exciplex PL in the bilayer structure (Fig. 1) and in the doped layer (Fig. 4) clearly indicate that ET from high-energy exciplexes to low-energy exciplexes takes place, resulting in the diffusion of exciplexes.

B. ET kinetics

To ensure that ET from the high-energy exciplex to the low-energy exciplex in film B can describe their transient decay profiles quantitatively, we fit the transient PL profiles for the TCTA/m-MTDATA/PO-T2T mixed film (m.r. 5:5:90), as shown in Figs. 6(a) and 6(b), using the following equations:

$$\frac{d[(T/P)^*]}{dt} = -k_p^{T/P}[(T/P)^*] - k_{ET}[(T/P)^*], \quad (1)$$

$$\frac{d[(m/P)^*]}{dt} = -k_p^{m/P}[(m/P)^*] + k_{ET}[(T/P)^*], \quad (2)$$

where $[(T/P)^*]$ and $[(m/P)^*]$ are the concentrations of the singlet TCTA/PO-T2T exciplexes $[(T/P)^*]$ exciplexes) and singlet m-MTDATA/PO-T2T exciplexes $[(m/P)^*]$ in film B, respectively; $k_p^{T/P}$ and k_{ET} are the prompt decay rate constant of the $(T/P)^*$ in the TCTA/PO-T2T film and the ET rate constant from the $(T/P)^*$ to the $(m/P)^*$ in film B, respectively; and $k_p^{m/P}$ is the prompt decay rate constant of the $(m/P)^*$ in the m-MTDATA/PO-T2T film. We analyze only the transient PL profiles in the prompt region for the TCTA/m-MTDATA/PO-T2T system because the triplet-triplet ET from the $(T/P)^*$ to the m-MTDATA exciton, as well as to the $(m/P)^*$, can occur considering their energy levels, as shown in Fig. 4, which complicates the analysis.

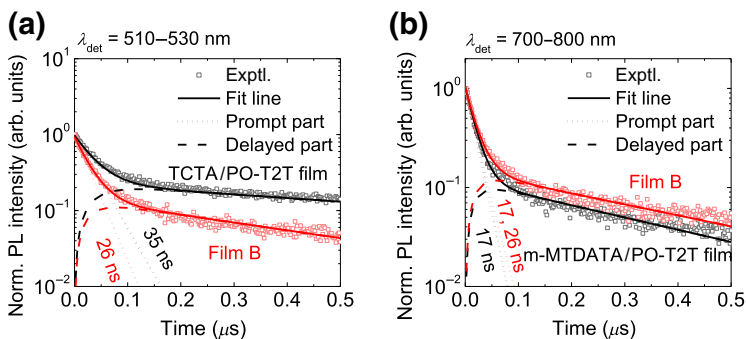


FIG. 6. (a) Normalized transient PL intensities (empty squares); fit lines of the total (solid lines), prompt (dotted line), and delayed (dashed line) parts for TCTA/PO-T2T film (m.r. 5:95) and film B in the wavelength range of 510 to 530 nm (semilogarithmic plot). The decay time constants for the prompt parts are also given. (b) Those for the m-MTDATA/PO-T2T (m.r. 5:95) film and film B in the wavelength range of 700 to 800 nm (semilogarithmic plot). The decay time constants for the prompt parts are also given.

The normalized solutions of the differential rate equations are

$$I_p^{T/P} = e^{-(k_p^{T/P} + k_{ET})t}, \quad (3)$$

$$I_p^{m/P} = \frac{k_p^{m/P} - k_p^{T/P} - (1 + C_0^{T/P}/C_0^{m/P})k_{ET}}{k_p^{m/P} - k_p^{T/P} - k_{ET}} e^{-k_p^{m/P}t} + \frac{(C_0^{T/P}/C_0^{m/P})k_{ET}}{k_p^{m/P} - k_p^{T/P} - k_{ET}} e^{-(k_p^{m/P} + k_{ET})t}, \quad (4)$$

where $(C_0^{T/P}/C_0^{m/P})$ is the initial concentration ratio of $(T/P)^*$ to $(m/P)^*$. It is interesting to note that the prompt part of $(T/P)^*$ in film B is a single-exponential line with a decay time constant of $1/(k_p^{T/P} + k_{ET})$ and that of $(m/P)^*$ in film B is a two-exponential line with decay time constants of $1/k_p^{m/P}$ and $1/(k_p^{m/P} + k_{ET})$, respectively.

There are four parameters in Eqs. (3) and (4): $(C_0^{T/P}/C_0^{m/P})$, $k_p^{T/P}$, $k_p^{m/P}$, and k_{ET} . $(C_0^{T/P}/C_0^{m/P})$ is set as 2/5, considering the extinction coefficients of TCTA and m-MTDATA at the excitation wavelength of 337 nm and the singlet-singlet ET from the TCTA exciton to the m-MTDATA exciton, by virtue of considerable spectral overlap between the TCTA emission spectrum and the m-MTDATA absorption spectrum, as shown in Fig. 5. The remaining three parameters, $k_p^{T/P}$, $k_p^{m/P}$, and $(k_p^{T/P} + k_{ET})$, are extracted by fitting the three transient PL profiles for $(T/P)^*$ in the TCTA/PO-T2T film, $(m/P)^*$ in the m-MTDATA/PO-T2T film, and $(T/P)^*$ in film B (TCTA/m-MTDATA/PO-T2T film), using a biexponential decay model, considering the TADF of the exciplexes, as follows [4,32], because the prompt part of the three transient decays are expected to show single exponential decays,

$$I_{\text{norm.PL}}(t) = I_p(t) + I_d(t) = e^{-k_p t} + C_d(e^{-k_d t} - e^{-k_p t}), \quad (5)$$

where t is the time after excitation; $I_{\text{norm.PL}}(t)$, $I_p(t)$, and $I_d(t)$ are the normalized transient PL intensity, prompt transient PL intensity, and delayed transient PL intensity from exciplexes, respectively; k_p and k_d are the prompt and delayed decay rate constants, respectively; and C_d is the pre-exponential constant for the delayed decay. $(1 - C_d)$

corresponds to the pre-exponential constant for the single-exponential prompt decay term (C_p) for the normalized transient PL intensity. The three transient PL profiles are fitted very well using Eq. (5), as represented by solid lines in Figs. 6(a) and 6(b), except the transient PL profile of $(m/P)^*$ in film B in Fig. 6(b). The extracted fitting parameters are summarized in Table I. The extracted k_{ET} value is $9.7 \times 10^6 \text{ s}^{-1}$.

The transient PL profile of $(m/P)^*$ in film B is fitted using Eq. (4) and the extracted parameters in Table I. The fitting results are shown in Fig. 6(b) for the normalized PL profile (solid line), along with the prompt (dotted line) and delayed parts (dashed line). The prompt part of $(m/P)^*$ in film B is a two-exponential line with decay time constants of 17 and 26 ns, which are $1/k_p^{m/P}$ and $1/(k_p^{m/P} + k_{ET})$, respectively. From the tail fitting for the delayed part of $(m/P)^*$ in film B (dashed line), the fit line of the entire transient PL profile for $(m/P)^*$ in film B (solid line) matches well with the experimental values, as shown in Fig. 6(b). Because of the larger number of $(m/P)^*$ than that of $(T/P)^*$ in film B at the excitation moment, the pre-exponential constants for the decay time constants of 17 and 26 ns in Eq. (4) are 0.81 and 0.19, respectively, leading to a smaller change of the transient PL profiles for $(m/P)^*$ than those for $(T/P)^*$. The very good fittings using the ET model confirm that ET takes place indeed from $(T/P)^*$ to $(m/P)^*$.

C. Concentration-dependent ET rate

To investigate the relationship between the ET rate constant and the distance between the energy donor and acceptor, we conduct concentration-dependent exciplex-quenching experiments with various molar ratios. A total of 16 films (doped films) are fabricated: eight TCTA/PO-T2T films with molar ratios of $x/100 - x$ and eight TCTA/m-MTDATA/PO-T2T films with molar ratios of $x/x/100 - 2x$, respectively, where $x = 3.0, 3.5, 4.0, 4.5, 5.0, 5.5, 6.0,$ and 6.5 . The thickness of the films is 50 nm. The doping concentrations of the films are kept low to maintain identical local environments for the dopants and ensure that the photophysical characteristics of the TCTA/PO-T2T exciplex are not influenced by the addition of m-MTDATA molecules. The transient PL intensities (semilogarithmic plots) of the films are shown in Fig. 7. The transient PL profiles are fitted by a biexponential

TABLE I. Fitting parameters for the normalized transient PL profiles of the TCTA/PO-T2T exciplexes in the TCTA/PO-T2T film and film B and those of the m-MTDATA/PO-T2T exciplexes in the m-MTDATA/PO-T2T film and film B.

Detection wavelength	Film	C_p	k_p (s^{-1})	k_d (s^{-1})
510–530 nm	TCTA/PO-T2T	0.77	2.84×10^7	1.09×10^6
	film B	0.85	3.81×10^7	2.36×10^6
700–800 nm	m-MTDATA/PO-T2T	0.89	5.80×10^7	2.85×10^6
	film B	0.70	5.80×10^7	2.56×10^6
		0.16	3.81×10^7	

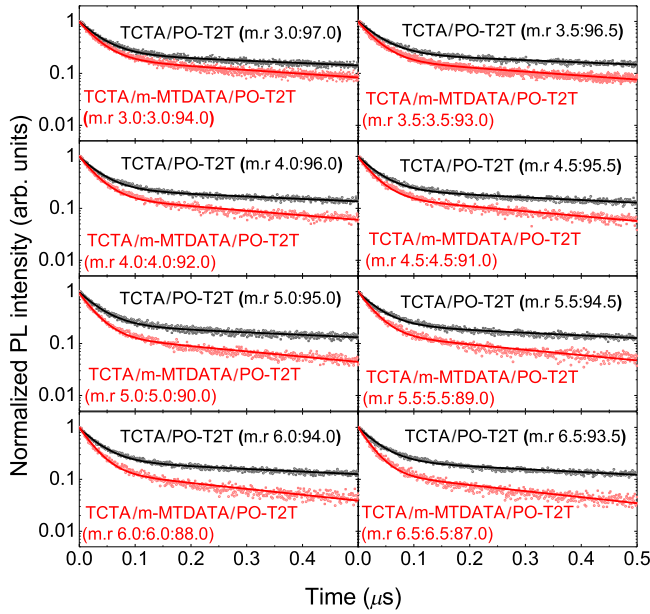


FIG. 7. Normalized transient PL intensities on a semilogarithmic scale in the wavelength range 510 to 530 nm, where the PL of the TCTA/PO-T2T exciplex is dominant in TCTA/PO-T2T and TCTA/m-MTDATA/PO-T2T films with various molar ratios (points) and fit lines by a two-exponential decay model (line) using the parameters in Table II.

decay model using Eq. (5), as described before, to extract the k_{ET} values. The transient behaviors of the TCTA/PO-T2T exciplexes in the TCTA/m-MTDATA/PO-T2T films with different doping concentrations are well fitted by the biexponential decays, and the fitting parameters are summarized in Table II. The prompt decay rate constants of the TCTA/PO-T2T exciplexes in the TCTA/PO-T2T films do not change much with different doping concentrations. In contrast, the prompt decay rate constants of the TCTA/PO-T2T exciplexes in the TCTA/m-MTDATA/PO-T2T films increase significantly with the doping concentration. The k_{ET} values are the difference between the prompt decay rate

constants of TCTA/PO-T2T exciplexes in the TCTA/PO-T2T and TCTA/m-MTDATA/PO-T2T mixed films with the same TCTA concentrations as those described in Sec. III B. The k_{ET} values are plotted in the semilogarithmic plot against $C_{m\text{-MTDATA}}^{-1/3}$ in Fig. 8(a). The ET rate constant decreases with the separation between the high-energy exciplex and the low-energy exciplex.

IV. DISCUSSION OF ET MECHANISMS

Experimental results shown in Sec. III clearly indicate that ET takes place between exciplexes. However, it seems to be counterintuitive, since the exciplex is generally thought to be formed through CT only in the excited state between donor and acceptor molecules at photoexcitation, and direct CT absorption from the ground state to the exciplex states does not take place. Therefore, the ET process must be carefully analyzed before we conclude that “direct” ET between exciplex states indeed takes place. The direct ET is ET from energy donors to energy acceptors without the generation of any other species, other than the energy acceptors, during the process of ET. There are two mechanisms for direct ET: FRET and DET. Both mechanisms require CT absorption from the ground state to the exciplex state for exciplex-exciplex ET. To investigate whether there is CT absorption in the exciplex, we select the TCTA/m-MTDATA/PO-T2T system and measure the CT absorption of the energy-accepting exciplex (m-MTDATA/PO-T2T). Figure 8(b) shows the extinction coefficients of a m-MTDATA/PO-T2T (m.r. 1:1) mixed film, along with the extinction coefficients of TCTA, m-MTDATA, and PO-T2T neat films [31]. The exciplex-forming mixed film only shows a clear absorption in the subband-gap region at a longer wavelength than 420 nm, even though it is very weak. Thick films are used for the purpose of detecting the intermolecular CT absorption by a simple absorption experiment of reflection-transmission measurement. Then, the absorbance for the exciplex-forming mixed film in the subband-gap wavelength region is analyzed using the transfer-matrix method

TABLE II. Pre-exponential constants and decay rate constants for the prompt and delayed decays of transient PL intensities in the wavelength range 510 to 530 nm, where the PL of the TCTA/PO-T2T exciplex is dominant in TCTA/PO-T2T and TCTA/m-MTDATA/PO-T2T films with various molar ratios and the corresponding ET rate constants.

Molar ratio of m-MTDATA	TCTA/PO-T2T			TCTA/m-MTDATA/PO-T2T			k_{ET} [10^6 s $^{-1}$]
	C_p	k_p [10^6 s $^{-1}$]	k_d [10^6 s $^{-1}$]	C_p	k_p [10^6 s $^{-1}$]	k_d [10^6 s $^{-1}$]	
3.0	0.76	27.7 ± 1.1	1.04 ± 0.03	0.81	32.9 ± 1.5	1.60 ± 0.07	5.2 ± 0.9
3.5	0.76	27.0 ± 0.4	0.99 ± 0.04	0.82	33.3 ± 0.7	1.78 ± 0.06	6.3 ± 0.4
4.0	0.76	28.8 ± 0.9	1.08 ± 0.04	0.84	35.7 ± 0.5	2.05 ± 0.07	6.9 ± 0.5
4.5	0.77	29.4 ± 0.1	1.17 ± 0.08	0.83	36.8 ± 0.4	2.18 ± 0.18	7.4 ± 0.2
5.0	0.77	28.4 ± 1.0	1.09 ± 0.01	0.85	38.1 ± 0.5	2.36 ± 0.04	9.7 ± 0.6
5.5	0.76	29.0 ± 2.2	1.18 ± 0.01	0.85	38.4 ± 0.5	2.39 ± 0.15	9.5 ± 1.1
6.0	0.75	29.1 ± 0.4	1.16 ± 0.05	0.86	40.1 ± 0.3	2.65 ± 0.14	11.0 ± 0.3
6.5	0.78	29.3 ± 3.0	1.23 ± 0.08	0.87	42.5 ± 2.8	2.74 ± 0.21	13.2 ± 2.1

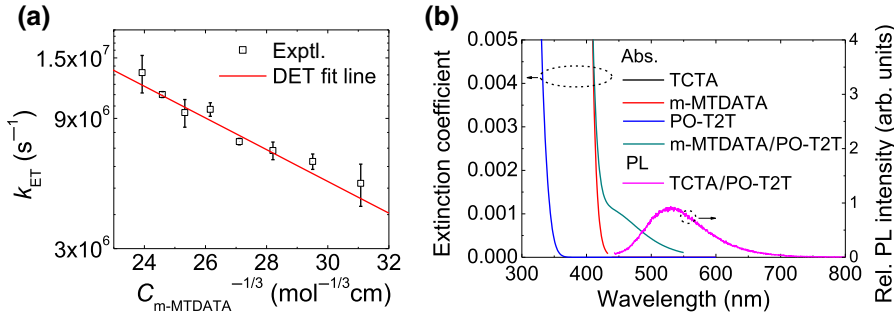


FIG. 8. (a) Plot of experimental values (squares) of the logarithm scale of k_{ET} versus $C_{m-MTDATA}^{-1/3}$ and a DET fit line (solid line). (b) The extinction coefficient of TCTA, m-MTDATA, PO-T2T, and m-MTDATA/PO-T2T (m.r. 1:1) films below 0.005, and the time-resolved PL spectra integrated for 500 ns after excitation of TCTA/PO-T2T (m.r. 5:95) film.

to obtain an extinction coefficient for the intermolecular CT state as low as 10^{-4} . Details are described in Ref. [31].

The indirect ET mechanisms are also considered for ET from the high-energy exciplex to the low-energy exciplex. The indirect ET could have polaron pairs as intermediate products during the process of ET, which is different from that of direct ET. Polaron pairs could be generated by exciplex dissociation and they could recombine into exciplexes, apart from the dissociated exciplex in various ways. The Langevin recombination, trap-assisted recombination, and geminate recombination are considered in this section. Recently, indirect ET via geminate recombination is reported as the inchworm mechanism [19].

A. DET

DET can be considered as a mechanism for ET, considering that the extinction coefficient of the CT absorption for the exciplexes is very small, in the order of 10^{-3} . We consider DET between the nearest energy-donating exciplex (TCTA/PO-T2T exciplex) and energy-accepting exciplex (m-MTDATA/PO-T2T exciplex), and ET between more separated pairs is ignored because the DET rate constant decreases exponentially with the separation distance as follows [33]:

$$k_{DET} = NKJ \exp(-\beta R), \quad (6)$$

where k_{DET} is the DET rate constant, N is the number of nearest energy-accepting species with a separation of R , K is the experimental factor related to the specific orbital interactions, J is the spectral overlap integral normalized for the molar extinction coefficient of the energy-accepting species, and β is the attenuation factor arising from the electronic exchange integral that is considered to drop exponentially in the tail of molecular orbitals [34,35]. The nearest distances between the TCTA/PO-T2T exciplexes and the m-MTDATA/PO-T2T exciplexes in the mixed films are calculated using Eq. (7) in the Wigner–Seitz approximation [36], where TCTA and m-MTDATA molecules doped in bulk PO-T2T at low

concentrations are assumed to be uniformly dispersed:

$$\frac{4}{3}\pi\left(\frac{R}{2}\right)^3 = \left(\frac{N_d}{N_A}\right)^{-1} = (2N_A C_{m-MTDATA})^{-1}, \quad (7)$$

where R (in units of cm) is the distance between the nearest TCTA/PO-T2T exciplexes and m-MTDATA/PO-T2T exciplex, which corresponds to the distance between TCTA and m-MTDATA molecules in this system; N_d is the number of dopants in a volume of V ; N_A is the Avogadro number; and $C_{m-MTDATA}$ is the molar concentration of m-MTDATA in the TCTA/m-MTDATA/PO-T2T mixed film (in units of mol cm⁻³) calculated from the molar ratio of mixed films under the assumption that all films have a density of 1 g cm⁻³. The grazing-incident small-angle x-ray scattering (GISAXS) is measured for the mixed film with the highest doping concentration [TCTA/m-MTDATA/PO-T2T (m.r. 6.5:6.5:87) film] to investigate whether the dopant molecules form aggregates or not. Figure 9(a) shows the GISAXS image for the film, and the horizontal line cut of the image is shown in Fig. 9(b), which is a semilogarithmic plot. The GISAXS image is measured for 5 s, and x-rays with an energy of 11.57 keV are incident with an angle of 0.15° relative to the surface of the film. A “Guinier knee” is not observed in the horizontal line cut. This indicates that doping molecules do not form aggregates in the film [37,38].

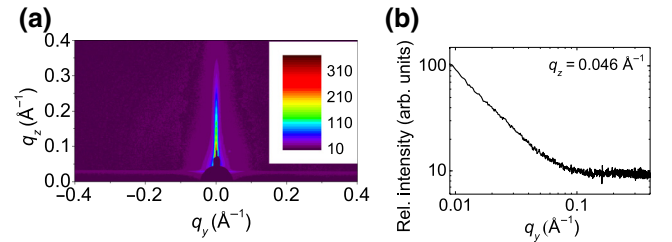


FIG. 9. (a) GISAXS image measured for TCTA/m-MTDATA/PO-T2T (m.r. 6.5:6.5:87) films. (b) Horizontal GISAXS line cut of TCTA/m-MTDATA/PO-T2T (m.r. 6.5:6.5:87) film at $q_z = 0.046$ Å⁻¹ (semilogarithmic plot).

Substituting Eq. (7) into Eq. (6) results in

$$\log_{10} k_{\text{DET}} = \log_{10}(NKJ) - \frac{\beta}{2.303} \left(\frac{3}{\pi N_A} \right)^{1/3} C_{\text{m-MTDATA}}^{-1/3}. \quad (8)$$

The linear fit line of k_{ET} against $C_{\text{m-MTDATA}}^{-1/3}$ in the semilogarithmic plot in Fig. 8(a) indicates that the ET rate constant decreases exponentially with the distance between the TCTA/PO-T2T exciplex and the m-MTDATA/PO-T2T exciplex in mixed films, demonstrating that ET takes place by DET. The attenuation factor arising from the electronic exchange integral is 1.1 nm^{-1} and the pre-exponential constant is $NKJ = 2.9 \times 10^8 \text{ s}^{-1}$ from the fitting with Eq. (8). Zhang and Forrest report that the diffusion of the triplet excited states of phosphors takes place via a Dexter-type exchange mechanism [39]. DET between the phosphors has attenuation factors of $1.2\text{--}1.5 \text{ nm}^{-1}$ and pre-exponential constants of $6.4 \times 10^6 \text{ s}^{-1}\text{--}3.0 \times 10^8 \text{ s}^{-1}$, which are similar values to those of our results [39]. It indicates that ET between the exciplexes also takes place by a Dexter-type exchange mechanism in organic films. The DET process from exciplexes to exciplexes can be explained using a molecular-orbital diagram, as schematically represented in Fig. 10(a), to explain the exchange mechanism.

There are two requirements for DET to take place by the Fermi golden rule. One is spectral overlap between the absorption of energy acceptors and emission of energy donors, which is satisfied in the exciplex systems, as discussed at the beginning of Sec. IV. The other one is the electronic exchange integral between energy-donor states and energy-acceptor states. The electronic exchange integral drops exponentially with the separation between them. Because of this reason, DET is thought to occur only when the energy donor and acceptor are in physical contact [34]. However, physical contact is not always a necessary condition for efficient long-range DET to occur, and long-range DETs without physical contact have been reported, known as the superexchange ET, which is the exchange ET with

the influence of intervening states [35,39,40]. The large coupling between π -conjugated molecules could expand the exchange integral between them to large separation, when the energy donor and acceptor are π -conjugated molecules in the π -conjugated medium. It indicates that physical contact between the energy donor and acceptor is not a necessary condition for DET.

Long-range DET with small attenuation factors of around 1 nm^{-1} can be explained by the state energy diagram shown in Fig. 10(b) [40–43], where v_1 , v , and v_2 are the electronic exchange integrals between the states of the energy-donating exciplex and medium molecule, between the states of the medium molecules, and between the states of the medium molecule and the energy-accepting exciplex, respectively. As a result of the first-order perturbation theory, V_{total} is the superexchange electronic exchange integral, which is the indirect electronic exchange integral via intermediate states (medium states) [35,39,42,43]. The small β in organic π -conjugated films can be explained by large coupling between π -conjugated molecules, according to the McConnell relationship [35,39,41–43]. According to this theory, β can be expressed by [41–43]

$$\beta = \frac{2}{R_0} \ln \left| \frac{\Delta}{v} \right|, \quad (9)$$

where R_0 is the length of the repeating units between energy donors and acceptors, Δ is the energy difference between the energy-donor states and localized states of the repeating units, and v is the exchange integral between the repeating units. Eq. (9) indicates that a large v could lead to a decrease in β , i.e., the large coupling between excitonic states of small π -conjugated molecules could increase the possibility of DET between an energy donor and an energy acceptor with large separation. When the electronic exchange integrals between π -conjugated molecules are negligible, the electronic exchange integral for the superexchange ET becomes negligible, resulting in large β requiring direct physical contact [2,43]. Therefore, the small β in exciplex-forming blended films must be caused by large coupling between π -conjugated molecules, according to McConnell relationship.

Other mechanisms are also considered for the ET process. However, ET rate constants of other mechanisms are negligible compared with those of the exchange mechanism in the system investigated in this study as follows.

B. FRET

The FRET rate constant (k_{FRET}) can be expressed by [44]

$$k_{\text{FRET}} = \frac{9000 \ln 10 N_R k^2 k_r}{128 \pi^5 N_A n^4} \frac{\int I_D(\lambda) \varepsilon_A(\lambda) \lambda^4 d\lambda}{\int I_D(\lambda) d\lambda} \frac{1}{R^6}, \quad (10)$$

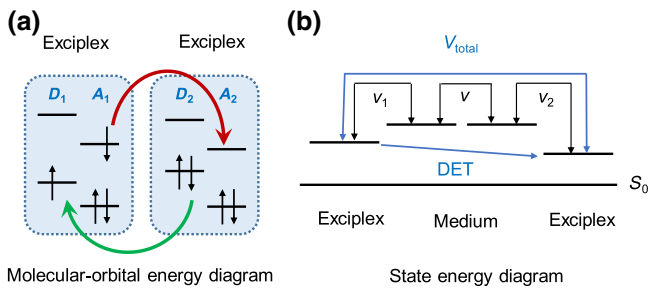


FIG. 10. (a) Schematic molecular-orbital energy diagrams of DET from an exciplex to an exciplex. (b) Schematic state energy diagrams of DET from an exciplex to an exciplex in π -conjugated molecular films.

where k_{FRET} is the FRET rate constant, N_R is the number of energy acceptors with a separation of R from an energy donor, κ^2 is the dipole orientation factor, k_r is the radiative rate constant of the energy-donating states, n is the refractive index of the medium, λ is the wavelength (in units of cm), I_D is the emission spectrum of the energy-donating states, ε_A is the molar extinction coefficient of energy-accepting states (in units of $\text{l cm}^{-1} \text{mol}^{-1}$), and R is the distance between the energy donors and acceptors (in units of cm). Based on the assumption that TCTA and m-MTDATA molecules doped into the bulk of PO-T2T molecules at low concentrations are uniformly dispersed in the Wigner-Seitz approximation [36], the number of the nearest energy-accepting species is six in TCTA/m-MTDATA/PO-T2T doped films. Again, we consider only FRET between the nearest energy-donating exciplex and energy-accepting exciplex because FRET between the second-nearest-energy donor-acceptor pairs would be more than 10 times smaller. The dipole orientation factor is assumed to be $2/3$ for randomly oriented energy donors and energy acceptors. The refractive index of the medium of TCTA/m-MTDATA/PO-T2T doped films is determined to be 1.73, which is the same as the refractive index of PO-T2T neat films at a wavelength of 500 nm. The nearest distance between the TCTA/PO-T2T exciplexes and the m-MTDATA/PO-T2T exciplexes can be calculated from Eq. (7). The emission spectrum of the TCTA/PO-T2T singlet exciplex is depicted in Fig. 8(b). The molar extinction coefficient of the m-MTDATA/PO-T2T singlet exciplex (in units of $\text{l cm}^{-1} \text{mol}^{-1}$) can be obtained by

$$\varepsilon_A = \frac{4\pi\kappa}{\lambda} C_{\text{m-MTDATA}}^{-1} = \frac{4\pi\kappa M_w}{1000\lambda\rho_{\text{film}}}, \quad (11)$$

where κ is the extinction coefficient of m-MTDATA/PO-T2T singlet exciplexes, as shown in Fig. 8(b) [31]; ρ_{film} is the density of the film (in units of g cm^{-3}); and M_w is the sum of molecular weights of m-MTDATA and PO-T2T (in units of g mol^{-1}) for the m-MTDATA/PO-T2T (m.r. 1:1) film. All films are assumed to have a density of 1 g cm^{-3} . The k_r of the TCTA/PO-T2T singlet exciplex can be derived from the two-exponential decay model for TADF emission [4]:

$$k_r = k_p \Phi_{\text{PL}} \frac{\int_0^\infty I_p(t) dt}{\int_0^\infty I_{\text{norm.PL}}(t) dt}, \quad (12)$$

where k_r and k_p are the fluorescence rate constant and prompt decay rate constant of exciplexes, respectively, and Φ_{PL} is the PL quantum yield (PLQY) of exciplexes. The PLQY of the TCTA/PO-T2T exciplexes is measured to be 35%. The k_r of the TCTA/PO-T2T singlet exciplex is calculated to be $1.5 \times 10^6 \text{ s}^{-1}$ from Eq. (5) and the transient PL characteristics from the TCTA/PO-T2T

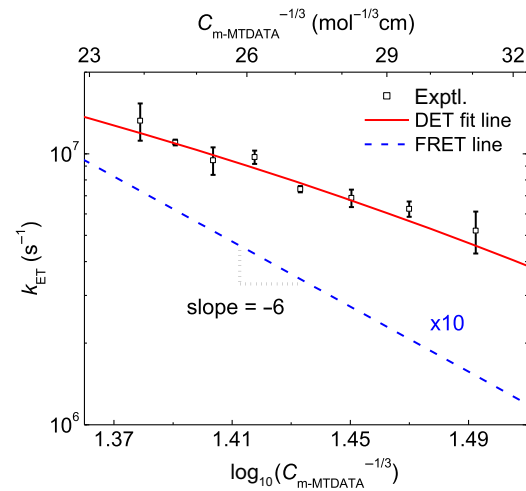


FIG. 11. Plot of experimental values (empty squares) of the logarithmic scale of k_{ET} versus $\log_{10}(C_{\text{m-MTDATA}}^{-1/3})$, a DET fit line (solid line), and calculated FRET rate constants ($\times 10$) from Eq. (10) (dashed line).

films are summarized in Table II. The calculated values of Eq. (10) on a logarithmic scale are plotted as dashed lines in Fig. 11. The FRET rate constants are almost one order of magnitude smaller than that of the experimental ET rate constants, which are fitted by the Dexter-type exchange mechanism. Not only that, the concentration dependence of the FRET rate constants does not follow the experimental data ($\propto R^{-6}$ for FRET vs $e^{-\beta R}$ for DET). The much smaller FRET rate constant of the exciplex can be understood from the very small extinction coefficient for CT absorption. These results reveal that FRET is not the dominant mechanism for exciplex diffusion.

C. Exciplex dissociation followed by Langevin recombination

We consider three indirect ET cases: exciplex dissociation followed by Langevin recombination, trap-assisted recombination, or geminate recombination. We first consider Langevin recombination, which is the recombination of free electrons and holes. Langevin recombination is a bimolecular process different from trap-assisted recombination or geminate recombination.

The mCBP/PO-T2T exciplexes and TCTA/PO-T2T exciplexes, which are the high-energy exciplexes in each system, can be dissociated into free polarons and they can recombine into low-energy exciplexes in the organic films. The transient behavior of the exciplex emission must depend on the density of the charged species at the moment of photoexcitation, since Langevin recombination is a bimolecular process. The initial numbers of free electrons and holes are both proportional to the intensity of the excitation light. The square dependence of the exciplex generation rate will result in the excitation intensity

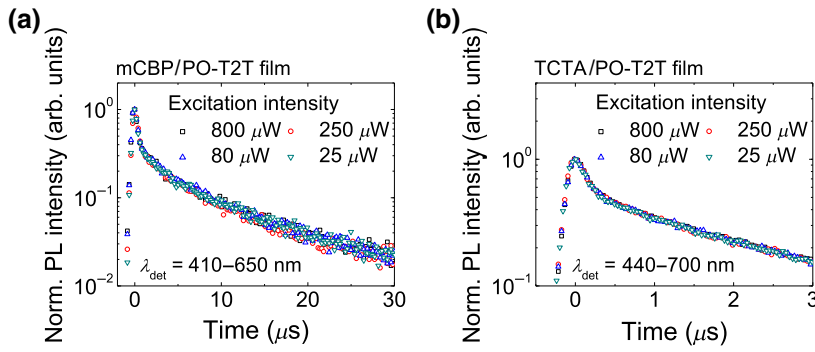
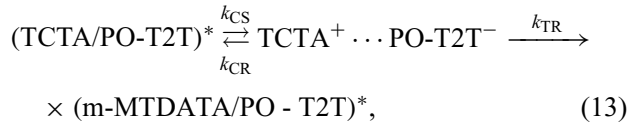


FIG. 12. (a) Normalized transient PL profiles of mCBP/PO-T2T film (m.r. 1:1) excited by a 337 nm pulsed laser light (N_2 laser) at different intensities in the wavelength range of 410 to 650 nm (semilogarithmic plot). (b) Those of TCTA/PO-T2T film (m.r. 5:95) at different intensities in the wavelength range of 440 to 700 nm (semilogarithmic plot).

dependence of decay rate constants if Langevin recombination is a dominant process for the generation of the singlet exciplex states. The transient PL profiles for the mCBP/PO-T2T film (m.r. 1:1) and TCTA/PO-T2T film (m.r. 5:95), where the high-energy exciplexes for each system exist, exhibit negligible change with different excitation light intensities, as shown in Figs. 12(a) and 12(b), respectively, which are semilogarithmic plots. The excitation light intensities are controlled by neutral density filters with different optical densities ranging from 25 to 800 μW . These results indicate that bimolecular recombination or Langevin recombination hardly participate in the decay of exciplexes to ground states.

D. Exciplex dissociation followed by trap-assisted recombination

Indirect ETs via unimolecular recombination are also considered. However, the small dissociation rate constant of exciplexes leads to the small indirect ET rate constants, which are negligible compared with the experimental ET rate constants. Indirect ET via trap-assisted recombination of polarons formed by the dissociation of exciplexes is considered first. The TCTA/PO-T2T exciplexes dissociate into polarons and then trap-assisted recombination occurs to form the m-MTDATA/PO-T2T exciplexes:



k_{CS} , k_{CR} , and k_{TR} are the rate constants for exciplex dissociation, geminate recombination, and trap-assisted recombination, respectively. When a steady-state approximation for the concentrations of intermediates is applied,

$$\begin{aligned} k_{\text{CS}}[(\text{TCTA/PO-T2T})^*] - k_{\text{CR}}[\text{TCTA}^+ \cdots \text{PO-T2T}^-] \\ - k_{\text{TR}}[\text{TCTA}^+ \cdots \text{PO-T2T}^-] = 0, \end{aligned} \quad (14)$$

the quenching rate constant of TCTA/PO-T2T exciplexes in Eq. (14) can be expressed by

$$\begin{aligned} k_{\text{ET}}[(\text{TCTA/PO-T2T})^*] &= k_{\text{CS}}[(\text{TCTA/PO-T2T})^*] \\ &\quad - k_{\text{CR}}[\text{TCTA}^+ \cdots \text{PO-T2T}^-] \\ &= k_{\text{CS}} \left(1 - \frac{1}{k_{\text{TR}}/k_{\text{CR}} + 1} \right) [(\text{TCTA/PO-T2T})^*], \end{aligned} \quad (15)$$

k_{TR} in Eq. (15) can be expressed by [45]

$$k_{\text{TR}} = \frac{q\mu_n n_{\text{trap}}}{\varepsilon\varepsilon_0} = \frac{q\mu_n N_A C_{\text{m-MTDATA}}}{\varepsilon\varepsilon_0}, \quad (16)$$

where q is the elementary charge, μ_n is the electron mobility in the film (in units of $\text{cm}^2 \text{V}^{-1} \text{s}^{-1}$), n_{trap} is the density of the traps for holes corresponding to the density of m-MTDATA in the TCTA/m-MTDATA/PO-T2T mixed film, $C_{\text{m-MTDATA}}$ is the molar concentration of m-MTDATA in the films (in units of mol cm^{-3}), ε is the dielectric constant of the film, and ε_0 is the vacuum permittivity. We consider that m-MTDATA molecules behave as hole traps when the trap-assisted recombination engages in ET from the TCTA/PO-T2T exciplexes to the m-MTDATA/PO-T2T exciplexes in the TCTA/m-MTDATA/PO-T2T films, not only because m-MTDATA has higher HOMO levels than those of TCTA and PO-T2T, but also logically the positive polaron originating from TCTA must be trapped in m-MTDATA for ET to take place from the TCTA/PO-T2T exciplexes to the m-MTDATA/PO-T2T exciplexes by the trap-assisted recombination. Thus, we use the molecular density of m-MTDATA in the films as the trap density. For the TCTA/m-MTDATA/PO-T2T film with $\varepsilon = 4$ and $\mu_n = 1.2 \times 10^{-5} \text{ cm}^2/\text{V s}$ [26], Eq. (15) becomes

$$k_{\text{ET}} = k_{\text{CS}} \left(1 - \frac{1}{3.3 \times 10^{12}/k_{\text{CR}} C_{\text{m-MTDATA}} + 1} \right). \quad (17)$$

The values of k_{CS} and k_{CR} are not known for the TCTA/m-MTDATA/PO-T2T film. Instead of determining the values by experiment, we use approximate values taken from a similar exciplex system in the literature, where a 1:1 mixed film of m-MTDATA/tri[3-(3-pyridyl)

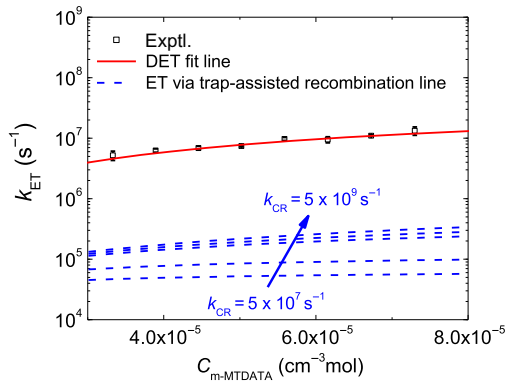


FIG. 13. Plot of experimental values (empty squares) of the logarithmic scale of k_{ET} versus $C_{m-MTDATA}$, a DET fit line (solid line), and possible lines of rate constants for ET via trap-assisted recombination [Eq. (17), when k_{CR} values are $5 \times 10^7 \text{ s}^{-1}$, $1 \times 10^8 \text{ s}^{-1}$, $5.3 \times 10^8 \text{ s}^{-1}$ [45], $1 \times 10^9 \text{ s}^{-1}$, and $5 \times 10^9 \text{ s}^{-1}$] (dashed line).

mesityl]borane (3TPYMB) is used as an exciplex-forming mixed film to report $k_{CS}/k_{CR} = 1.36 \times 10^{-3}$ and the binding energy of the m-MTDATA/3TPYMB exciplex of 0.17 eV [28]. If we assume the exciplex-binding energies in small-molecule π -conjugated organic films are similar, then $k_{CS}/k_{CR} = 1.36 \times 10^{-3}$ must be similar in both systems. Using the relationship, the k_{ET} values are calculated for different k_{CR} values of $5 \times 10^7 \text{ s}^{-1}$, $1 \times 10^8 \text{ s}^{-1}$, $5.3 \times 10^8 \text{ s}^{-1}$ [45], $1 \times 10^9 \text{ s}^{-1}$, and $5 \times 10^9 \text{ s}^{-1}$ and are compared with the experimental data and DET fitting in Fig. 13 on a semilogarithmic scale. The ET rate constants via trap-assisted recombination of polaron pairs generated from the dissociation of exciplexes are almost two orders of magnitude smaller than the experimental ET rate constants fitted by the Dexter-type exchange mechanism. Therefore, exciplex diffusion via trap-assisted recombination must be negligible relative to that of DET.

E. Exciplex dissociation followed by geminate recombination (inchworm mechanism)

Finally, we consider the inchworm mechanism of exciplex diffusion reported in Ref. [19] based on the magneto-PL observed from exciplex and Monte Carlo simulation, where an electron and a hole dissociate from an exciplex hop to neighboring molecules incoherently and recombine geminately. There are two arguments that lead us to think the inchworm mechanism will not be dominant in the exciplex-forming system. The first one is that the supporting data for explaining the inchworm mechanism are not powerful. The magnetic field data are used to support the inchworm mechanism. However, it should be noted that the interpretation of the magnetic-field effect in exciplexes is controversial at this moment [46,47]. Baldo *et al.* claim that the magnetic-field data for an exciplex can be explained

by the presence of polaron pairs in exciplex-forming films inducing hyperfine interaction (HFI) [19,28]. Splitting of T_+ and T_- can induce a decrease of the intersystem crossing rate by HFI when a magnetic field is applied. However, the magnetic-field response is too broad to explain the effect by the HFI. When applied magnetic fields are about one order of magnitude greater than the hyperfine coupling, intersystem crossing between T_{\pm} and S is shut off [48]. Considering that typical values of hyperfine coupling constants are 1–10 mT [48], the magnetic-field effect should saturate in the range of 10–100 mT. It is clearly shown in the magneto-electroluminescence of poly[2-methoxy-5-(2-ethylhexyloxy)-1,4-phenylenevinylene]- (MEH PPV) based OLEDs [47]. The magneto-electroluminescence of MEH PPV OLED devices at constant current saturates at about 100 mT, where the magnetic-field effect is governed by HFI [48]. On the other hand, the magnetic-field effect for exciplex reported by Baldo *et al.* saturates at about 300 mT and the full width at half maximum (FWHM) of the magnetic field effect is about 66 mT; these results are not easy to explain by the HFI between polaron pairs. Instead, Vardeny *et al.* analyze the magnetic-field effects on the PL of an exciplex by the Δg mechanism [47]. They also point out that the FWHM of the magnetic field effect on the PL of the exciplex of 32 mT is too large for the magnetic-field effect to originate from HFI. They conclude that magnetoreverse intersystem crossing between singlet and triplet exciplex states caused by the Δg mechanism will have a large contribution to the magnetic-field effect for the exciplex by analyzing the activation energy of the magnetic-field effect of the exciplex. Flatté, *et al.* also report that the Δg mechanism is dominant over HFI in the same system [49]. In addition, the magnetic-field effect is reported in TADF molecules (intramolecular CT molecules), where the dissociation of the exciton is barely expected, resulting in negligible density of polaron pairs inducing HFI [50]. The authors attribute the effect to spin-orbit coupling rather than HFI.

Second, the exciplex dissociation rate constant is too small to explain the large ET rate constant. The inchworm mechanism has three steps: dissociation of exciplexes into electrons and holes, incoherent hopping of the electrons and holes in a bound state, and geminate recombination of the electrons and holes. The processes are sequential, so that the slowest step must be the rate determining step. Baldo and co-workers report the rate constant for exciplex dissociation into the polaron pair as $7.2 \times 10^5 \text{ s}^{-1}$ and the geminate recombination of the polaron pairs as $5.3 \times 10^8 \text{ s}^{-1}$ [28]. Also, the geminate recombination rate constant in various organic electron donor-acceptor films are reported as 1×10^7 – $5 \times 10^9 \text{ s}^{-1}$ [22]. Given the exciplex binding energy of about 0.17 eV [28], the exciplex dissociation rate constant is in the range from 1×10^4 to $7 \times 10^6 \text{ s}^{-1}$. This implies that the ET rate constant via

the inchworm model must saturate to $7 \times 10^6 \text{ s}^{-1}$, regardless of how large the rate constant for charge hopping after exciplex dissociation is. This value is too small to explain our reported ET values with a maximum value of $1.3 \times 10^7 \text{ s}^{-1}$.

To sum up, we think that it may be a feasible mechanism, but it is too early to conclude that the magnetic-field effect on the PL of exciplexes is crucial evidence for the presence of a pair of an electron and a hole for the inchworm mechanism inducing HFI. Therefore, the inchworm mechanism is less likely to be a dominant mechanism in the exciplex-forming systems in this study, even though further studies are required to clarify whether the inchworm mechanism or trap-assisted mechanism can be applicable to this and other exciplex-forming systems, including the magnetic-field effect and the effect of inhomogeneity of the distribution of distances over which ET takes place in the doped amorphous films.

F. Exciplex-exciplex ET in OPVs

The DET process would also be dominant in polymer OPVs. We obtain a similar absorption coefficient for the intermolecular CT state in the m-MTDATA/PO-T2T mixed film [31] as those in the polymer/[6,6]-phenyl-C61-butyric acid methyl ester (PCBM) mixed films exploited in OPVs, as shown in Fig. 14 on a semilogarithmic scale [20]. Thus, the order of the FRET rate constant in the mixed film we investigate will be similar to that in the polymer/PCBM mixed films exploited in OPVs. The FRET rate constant is linearly proportional to both the radiative rate constant of an energy donor and spectral overlap with the molar extinction coefficient of an energy acceptor, as shown in Eq. (10). The order of magnitude of radiative rate constants of singlet exciplexes will be similar for small-molecule systems and polymer systems because the radiative rate constant is related to the extinction coefficient, according to the following equation based on one-dimensional oscillator theory [2]:

$$k_r = 3 \times 10^{-9} \bar{\nu}_0^2 \int \varepsilon d\bar{\nu}, \quad (18)$$

where k_r is the radiative rate constant, ε is the molar extinction coefficient, and $\bar{\nu}_0$ is the peak wave number for the molar extinction coefficient. Then, the order of magnitude of spectral overlap will also be similar because the attenuation coefficient for the CT state in the m-MTDATA/PO-T2T mixed film is similar to those in the polymer/PCBM mixed films, as shown in Fig. 14. Therefore, the DET must be considered for the exciplex-exciplex ET in OPVs, along with dissociation of CT states followed by geminated or nongeminated recombination.

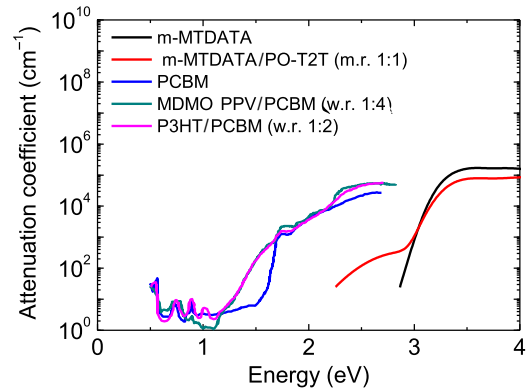


FIG. 14. Attenuation coefficients of m-MTDATA neat film, m-MTDATA/PO-T2T mixed film with a molar ratio of 1:1, PCBM neat film [20], poly[2-methoxy-5-(3',7'-dimethyloctyloxy)-1,4-phenylenevinylene] (MDMO PPV)/PCBM mixed film with a weight ratio (w.r.) of 1:4 [20], and poly(3-hexylthiophene-2,5-diyl) (P3HT)/PCBM mixed film with a weight ratio of 1:2 [20] (semilogarithmic plot).

V. CONCLUSION

It is demonstrated that there is ET from exciplexes to other kinds of exciplexes upon ET using time-resolved PL spectroscopy. ET from the high-energy exciplexes to the low-energy exciplexes is supported by the observation of the subband-gap CT absorption in exciplex-forming films to satisfy the necessary condition of spectral overlap between absorption and emission spectra for the ET process to take place. The ET can be explained by the superexchange mechanism based on the concentration-dependent ET rate constants. We conclude that DET could be the dominant mechanism for exciplex diffusion in our investigated exciplex-forming systems after investigating other possibilities. The diffusion mechanism must be widely applied to most optoelectronic materials in OLEDs and OPVs. As the importance of exciplexes or CT states in organic photonic devices, such as OLEDs and OPVs, has increased in recent years, the ET process discussed here must be taken into account and play an important role in understanding device characteristics and will contribute to the design of molecules and devices with improved performance. The result of ET is the generation of other kinds of exciplexes with different photophysical characteristics from the quenched exciplexes. This can be utilized for optoelectronic devices. Further studies are required to generalize the conclusion that DET is the dominant mechanism for exciplex diffusion.

ACKNOWLEDGMENTS

This work is supported by a grant from the National Research Foundation (NRF) funded by the Ministry of Science and ICT (MSIT).

S.W.L. and H.J.K. carried out the GISAXS measurement.

- [1] G. J. Kavarnos and N. J. Turro, Photosensitization by reversible electron transfer: Theories, experimental evidence, and examples, *Chem. Rev.* **86**, 401 (1986).
- [2] N. J. Turro, *Modern Molecular Photochemistry* (University Science Books, Sausalito, CA, USA, 1991).
- [3] J.-F. Wang, Y. Kawabe, S. E. Shaheen, M. M. Morrell, G. E. Jabbour, P. A. Lee, J. Anderson, N. R. Armstrong, B. Kippelen, E. A. Mash, and N. Peyghambarian, Exciplex electroluminescence from organic bilayer devices composed of triphenyldiamine and quinoxaline derivatives, *Adv. Mater.* **10**, 230 (1998).
- [4] K. Goushi, K. Yoshida, K. Sato, and C. Adachi, Organic light-emitting diodes employing efficient reverse intersystem crossing for triplet-to-singlet state conversion, *Nat. Photonics* **6**, 253 (2012).
- [5] Y.-S. Park, K.-H. Kim, and J.-J. Kim, Efficient triplet harvesting by fluorescent molecules through exciplexes for high efficiency organic light-emitting diodes, *Appl. Phys. Lett.* **102**, 153306 (2013).
- [6] X. K. Liu, Z. Chen, C. J. Zheng, C. L. Liu, C. S. Lee, F. Li, X. M. Ou, and X. H. Zhang, Prediction and design of efficient exciplex emitters for high-efficiency, thermally activated delayed-fluorescence organic light-emitting diodes, *Adv. Mater.* **27**, 2378 (2015).
- [7] Y. S. Park, W. I. Jeong, and J. J. Kim, Energy transfer from exciplexes to dopants and its effect on efficiency of organic light-emitting diodes, *J. Appl. Phys.* **110**, 124519 (2011).
- [8] S. Y. Kim, W. I. Jeong, C. Mayr, Y. S. Park, K. H. Kim, J. H. Lee, C. K. Moon, W. Brütting, and J. J. Kim, Organic light-emitting diodes with 30% external quantum efficiency based on a horizontally oriented emitter, *Adv. Funct. Mater.* **23**, 3896 (2013).
- [9] B. Zhao, T. Zhang, B. Chu, W. Li, Z. Su, H. Wu, X. Yan, F. Jin, Y. Gao, and C. Liu, Highly efficient red OLEDs using DCJTb as the dopant and delayed fluorescent exciplex as the host, *Sci. Rep.* **5**, 10697 (2015).
- [10] Y. Inai, M. Sisido, and Y. Imanishi, Distance and orientation dependence of electron transfer and exciplex formation of naphthyl and p-dimethyliamino groups fixed on a helical polypeptide chain, *J. Phys. Chem.* **94**, 6237 (1990).
- [11] I. R. Gould, S. Farid, and R. H. Young, Relationship between exciplex fluorescence and electron transfer in radical ion pairs, *J. Photochem. Photobiol. A -Chem* **65**, 133 (1992).
- [12] M. Bixon, J. Jortner, and J. W. Verhoeven, Lifetimes for radiative charge recombination in donor-acceptor molecules, *J. Am. Chem. Soc.* **116**, 7349 (1994).
- [13] I. R. Gould, R. H. Young, L. J. Mueller, a. C. Albrecht, and S. Farid, Electronic structures of exciplexes and excited charge-transfer complexes, *J. Am. Chem. Soc.* **116**, 8188 (1994).
- [14] J. W. Verhoeven, T. Scherer, B. Wegewijs, R. M. Hermant, J. Jortner, M. Bixon, S. Depaemelaere, and F. C. de Schryver, Electronic coupling in inter- and intramolecular donor-acceptor systems as revealed by their solvent-dependent charge-transfer fluorescence, *Rec. Trav. Chim. Pays Bas* **114**, 443 (1995).
- [15] A. C. Morteani, P. Sreearunothai, L. M. Herz, R. H. Friend, and C. Silva, Exciton Regeneration at Polymeric Semiconductor Heterojunctions, *Phys. Rev. Lett.* **92**, 247402 (2004).
- [16] Y. Huang, S. Westenhoff, I. Avilov, P. Sreearunothai, J. M. Hodgkiss, C. Deleener, R. H. Friend, and D. Beljonne, Electronic structures of interfacial states formed at polymeric semiconductor heterojunctions, *Nat. Mater.* **7**, 483 (2008).
- [17] D. Graves, V. Jankus, F. B. Dias, and A. Monkman, Photophysical investigation of the thermally activated delayed emission from films of m-MTDATA:PBD exciplex, *Adv. Funct. Mater.* **24**, 2343 (2014).
- [18] T. Strobel, C. Deibel, and V. Dyakonov, Role of Polaron Pair Diffusion and Surface Losses in Organic Semiconductor Devices, *Phys. Rev. Lett.* **105**, 266602 (2010).
- [19] P. B. Deotare, W. Chang, E. Hontz, D. N. Congreve, L. Shi, P. D. Reusswig, B. Modtland, M. E. Bahlke, C. K. Lee, A. P. Willard, V. Bulović, T. Van Voorhis, and M. A. Baldo, Nanoscale transport of charge-transfer states in organic donor-acceptor blends, *Nat. Mater.* **14**, 1130 (2015).
- [20] L. Goris, A. Poruba, L. Hod'Ákova, M. Vaněček, K. Haenen, M. Nešládek, P. Wagner, D. Vanderzande, L. De Schepper, and J. V. Manca, Observation of the subgap optical absorption in polymer-fullerene blend solar cells, *Appl. Phys. Lett.* **88**, 052113 (2006).
- [21] J. K. Klosterman, M. Iwamura, T. Tahara, and M. Fujita, Energy transfer in a mechanically trapped exciplex, *J. Am. Chem. Soc.* **131**, 9478 (2009).
- [22] T. M. Clarke and J. R. Durrant, Charge photogeneration in organic solar cells, *Chem. Rev.* **110**, 6736 (2010).
- [23] L. Goris, K. Haenen, M. Nešládek, P. Wagner, D. Vanderzande, L. De Schepper, J. D'haen, L. Luisen, and J. V. Manca, Absorption phenomena in organic thin films for solar cell applications investigated by photothermal deflection spectroscopy, *J. Mater. Sci.* **40**, 1413 (2005).
- [24] K. Vandewal, A. Gadisa, W. D. Oosterbaan, S. Bertho, F. Banishoeib, I. Van Severen, L. Lutsen, T. J. Cleij, D. Vanderzande, and J. V. Manca, The relation between open-circuit voltage and the onset of photocurrent generation by charge-transfer absorption in polymer: Fullerene bulk heterojunction solar cells, *Adv. Funct. Mater.* **18**, 2064 (2008).
- [25] K. Vandewal, S. Albrecht, E. T. Hoke, K. R. Graham, J. Widmer, J. D. Douglas, M. Schubert, W. R. Mateker, J. T. Bloking, G. F. Burkhard, A. Sellinger, J. M. J. Fréchet, A. Amassian, M. K. Riede, M. D. McGehee, D. Neher, and A. Salleo, Efficient charge generation by relaxed charge-transfer states at organic interfaces, *Nat. Mater.* **13**, 63 (2014).
- [26] W. Y. Hung, G. C. Fang, S. W. Lin, S. H. Cheng, K. T. Wong, T. Y. Kuo, and P. T. Chou, The first tandem, all-exciplex-based WOLED, *Sci. Rep.* **4**, 1 (2015).
- [27] J.-H. Lee, S.-H. Cheng, S.-J. Yoo, H. Shin, J.-H. Chang, C.-I. Wu, K.-T. Wong, and J.-J. Kim, An exciplex forming host for highly efficient blue organic light emitting diodes with low driving voltage, *Adv. Funct. Mater.* **25**, 361 (2015).
- [28] E. Hontz, W. Chang, D. N. Congreve, V. Bulović, M. A. Baldo, and T. Van Voorhis, The role of electron-hole separation in thermally activated delayed fluorescence in donor-acceptor blends, *J. Phys. Chem. C* **119**, 25591 (2015).
- [29] K. H. Kim, S. J. Yoo, and J. J. Kim, Boosting triplet harvest by reducing nonradiative transition of exciplex toward fluorescent organic light-emitting diodes with 100% internal quantum efficiency, *Chem. Mater.* **28**, 1936 (2016).

- [30] W. Y. Hung, P. Y. Chiang, S. W. Lin, W. C. Tang, Y. T. Chen, S. H. Liu, P. T. Chou, Y. T. Hung, and K. T. Wong, Balance the carrier mobility to achieve high performance exciplex OLED using a triazine-based acceptor, *ACS Appl. Mater. Interfaces* **8**, 4811 (2016).
- [31] H.-B. Kim and J.-J. Kim, A simple method to measure intermolecular charge-transfer absorption of organic films, *Org. Electron. Phys. Mater. Appl.* **62**, 511 (2018).
- [32] M. a Baldo and S. R. Forrest, Transient analysis of organic electrophosphorescence: I. Transient analysis of triplet energy transfer, *Phys. Rev. B* **62**, 10958 (2000).
- [33] D. L. Dexter, A theory of sensitized luminescence in solids, *J. Chem. Phys.* **21**, 836 (1953).
- [34] S. Speiser, Photophysics and mechanisms of intramolecular electronic energy transfer in bichromophoric molecular systems: Solution and supersonic jet studies photophysics and mechanisms of intramolecular electronic energy transfer in bichromophoric molecular systems, *Chem. Rev.* **96**, 1953 (1996).
- [35] A. Harriman, A. Khatyr, R. Ziessel, and A. C. Bennis-ton, An unusually shallow distance-dependence for triplet-energy transfer, *Angew. Chem. Int. Ed.* **39**, 4287 (2000).
- [36] N. W. Ashcroft and N. D. Mermin, *Solid State Physics* (Rinehart and Winston, Holt, 1976).
- [37] J. M. Szarko, J. Guo, Y. Liang, B. Lee, B. S. Rolczynski, J. Strzalka, T. Xu, S. Loser, T. J. Marks, L. Yu, and L. X. Chen, When function follows form: Effects of donor copolymer side chains on film morphology and BHJ solar cell performance, *Adv. Mater.* **22**, 5468 (2010).
- [38] J. M. Szarko, J. Guo, B. S. Rolczynski, and L. X. Chen, Current trends in the optimization of low band gap polymers in bulk heterojunction photovoltaic devices, *J. Mater. Chem.* **21**, 7849 (2011).
- [39] Y. Zhang and S. R. Forrest, Triplet diffusion leads to triplet-triplet annihilation in organic phosphorescent emitters, *Chem. Phys. Lett.* **590**, 106 (2013).
- [40] B. Albinsson and J. Martensson, Excitation energy transfer in donor-bridge-acceptor systems, *Phys. Chem. Chem. Phys.* **12**, 7338 (2010).
- [41] H. M. McConnell, Intramolecular charge transfer in aromatic free radicals, *J. Chem. Phys.* **35**, 508 (1961).
- [42] M. P. Eng and B. Albinsson, Non-exponential distance dependence of bridge-mediated electronic coupling, *Angew. Chem. Int. Ed.* **45**, 5626 (2006).
- [43] B. Albinsson, M. P. Eng, K. Pettersson, and M. U. Winters, Electron and energy transfer in donor-acceptor systems with conjugated molecular bridges, *Phys. Chem. Chem. Phys.* **9**, 5847 (2007).
- [44] S. Pillai and P. C. Van der Vliet, *FRET and FLIM Techniques* (Elsevier, UK, Oxford, 2009).
- [45] M. Kuik, L. J. A. Koster, G. A. H. Wetzelaer, and P. W. M. Blom, Trap-assisted Recombination in Disordered Organic Semiconductors, *Phys. Rev. Lett.* **107**, 256805 (2011).
- [46] R. Geng, T. T. Daugherty, K. Do, H. M. Luong, and T. D. Nguyen, A review on organic spintronic materials and devices: I. Magnetic field effect on organic light emitting diodes, *J. Sci. Adv. Mater. Devices* **1**, 128 (2016).
- [47] T. Basel, D. Sun, S. Baniya, R. McLaughlin, H. Choi, O. Kwon, and Z. V. Vardeny, Magnetic field enhancement of organic light-emitting diodes based on electron donor-acceptor exciplex, *Adv. Electron. Mater.* **2**, 1500248 (2016).
- [48] I. R. Gould, N. J. Turro, and M. B. Zimmt, Magnetic field and magnetic isotope effects on the products of organic reactions, *Adv. Phys. Org. Chem.* **20**, 1 (1984).
- [49] Y. Wang, K. Sahin-Tiras, N. J. Harmon, M. Wohlgenannt, and M. E. Flatté, Immense Magnetic Response of Exciplex Light Emission Due to Correlated Spin-Charge Dynamics, *Phys. Rev. X* **6**, 011011 (2016).
- [50] B. Hu, Proc. SPIE 10362, 103620E (2017).